

# LINAC CODE BENCHMARKING WITH HIGH INTENSITY EXPERIMENTS AT THE UNILAC

L. Groening, W. Barth, W. Bayer, G. Clemente, L. Dahl, P. Forck, P. Gerhard,  
 I. Hofmann, M.S. Kaiser, M. Maier, S. Mickat, T. Milosic, G. Riehl, H. Vormann,  
 S. Yaramyshev, GSI, D-64291 Darmstadt, Germany  
 D. Jeon, SNS, ORNL, Oak Ridge, TN 37831, USA  
 D. Uriot, CEA IRFU, F-91191 Gif-sur-Yvette, France  
 R. Tiede, Goethe University, Frankfurt a.M., Germany

## Abstract

This paper is on benchmarking of four beam dynamics simulation codes, i.e. DYNAMION, PARMILA, TraceWin, and LORASR against systematic measurements of beam emittance growth for different machine settings. Experimental set-ups, data reduction, the preparation of the simulations, and the evaluation of the simulations will be described. It was found that the mean value of final horizontal and vertical rms-emittance can be reproduced well by the codes. Generally the accuracy decreases with the amount of mismatch. Additionally we report on the experimental evidence of the 4<sup>th</sup>-order space charge driven resonance at transverse phase advances around 90°.

## INTRODUCTION

In the last decades many beam dynamics computer codes were developed [1] in order to simulate emittance growth along a linac. Several benchmarking studies among codes have been performed [2, 3, 4] generally assuming idealized conditions as initial Gaussian distributions, equal transverse emittances, matched injection into a periodic lattice, and small longitudinal emittance with respect to the rf-bucket size. In case of an operating linac not all of these conditions are met. To apply simulation codes to a realistic environment a benchmark activity was started aiming at the simulations of beam emittance measurements performed at a DTL entrance and exit, respectively. The studies were performed at the GSI UNILAC [5]. For the simulations four different codes were used: DYNAMION [6], PARMILA [7], TraceWin [8], and LORASR [9].

The first benchmarking has been done with moderate mismatch with respect to the periodic DTL solution. The zero current transverse phase advance  $\sigma_o$  has been varied from 35° to 90°. A detailed description of this first campaign is given in [10]. A second campaign suggested in [11] aimed for exploration of the 90° stop-band by varying  $\sigma_o$  from 60° to 130°. In this campaign the mismatch was minimized in order to mitigate the effects of the envelope instability.

## EXPERIMENT SET-UP AND PROCEDURE

Intense beams were provided by a MUCIS source at low charge states with the energy of 2.2 keV/u. An RFQ followed by two IH-cavities (HSI section) accelerates the ions

to 1.4 MeV/u using an rf-frequency of 36 MHz. A subsequent gas-stripper increases the average charge state of the ion beam. Final acceleration to 11.4 MeV/u is done in the Alvarez DTL section operated at 108 MHz. The increase of rf-frequency by a factor of three requires a dedicated matching section preceding the DTL. It comprises a 36 MHz re-buncher for longitudinal bunch compression, a 108 MHz re-buncher for final bunch rotation, a quadrupole doublet for transverse compression, and a quadrupole triplet for final transverse beam matching.

The Alvarez DTL comprises five independent rf-tanks. Transverse beam focusing is performed by quadrupoles in the F-D-D-F mode. Each drift tube houses one quadrupole. The periodicity of the lattice is interrupted by four inter-tank sections, where D-F-D focusing is applied. Acceleration is done -30° from crest in the first three tanks and -25° from crest in the last two tanks.

Figure 1 presents the schematic set-up of the experiments. Beam current transformers are placed in front of

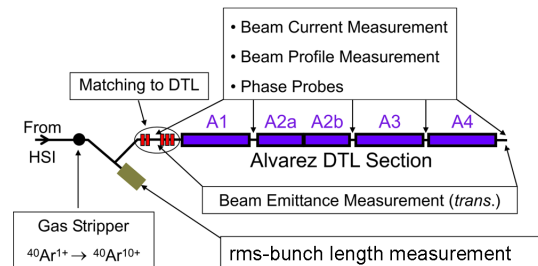


Figure 1: Schematic set-up of the experiments.

and behind the DTL as well as horizontal and vertical slit/grid emittance measurement devices. The total accuracy of each rms-emittance measurement including its evaluation is estimated to be 10%. A set-up to measure the longitudinal rms-bunch length is available in front of the DTL [12]. It measures the time of impact of a single ion on a foil. This time is related to a 36 MHz master oscillator. The resolution is 0.3° (36 MHz). Prior to the high intensity measurements a scan with very low beam current was done, demonstrating that no emittance growth occurs in absence of space charge forces. Afterwards the HSI was set to obtain 7.1 mA of  $^{40}\text{Ar}^{10+}$  in front of the DTL being space charge equivalent to the UNILAC design beam of 15 mA of  $^{238}\text{U}^{28+}$ . Horizontal and vertical phase space distributions were measured in front of the DTL. The lon-

itudinal rms-bunch length was measured at the entrance to the DTL. The DTL quadrupoles were set to the required zero current transverse phase advance  $\sigma_o$ . Due to space charge the phase advances in all three dimensions were depressed. The transverse depression reached from 14% (130°) to 43% (35°). Afterwards the quadrupoles and rebunchers preceding the DTL were set to obtain full transmission and to minimize low energy tails of the beam. For each value of  $\sigma_o$  horizontal and vertical beam emittances were measured at the exit of the DTL with a resolution of 0.8 mm in space and 0.5 mrad in angle.

Each emittance measurement delivers a two dimensional matrix of discrete slit-positions and discrete angles. The data are processed by the measurement & evaluation program PROEMI [13]. Simulations deliver a set of six dimensional particle coordinates. This ensemble is projected onto a pixel-grid having the same characteristics as the slit/grid device used for the measurements. The grid is read by the measurement evaluation program PROEMI such that data reduction was done in the same way as for measured data.

## INPUT FOR SIMULATIONS

The reconstruction of the initial distribution was done in two steps. First the rms-Twiss parameters were determined. In the second step the type of distribution was reconstructed. The transverse rms-measurements and the longitudinal rms-measurements on the initial distribution, done at different locations along the beam line (Fig. 2) were combined in a self-consistent way based on envelope tracking of rms-equivalent KV-distributions [10]. The recon-

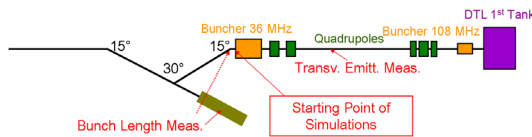


Figure 2: Matching section to the DTL including the reference points used for reconstruction of the initial phase space distribution.

struction of the type of distribution is based on evaluation of the brilliance curve, i.e. the fractional rms-emittance as function of the fraction. Different amounts of halo have been found in the two transverse plane. For proper modelling of the initial distribution, both brilliance curves must be reproduced simultaneously. This was achieved by using a distribution function as

$$f(R) = \frac{a}{2.5 \cdot 10^{-4} + R^{10}}, \quad R \leq 1 \quad (1)$$

and  $f(R)=0$  for  $R > 0$  with

$$R^2 = X^2 + X'^2 + Y^{1.2} + Y'^{1.2} + \Phi^2 + (\delta P/P)^2, \quad (2)$$

where  $a$  is the normalization constant and the constant in the denominator results from the cut off condition at  $R = 1$ .

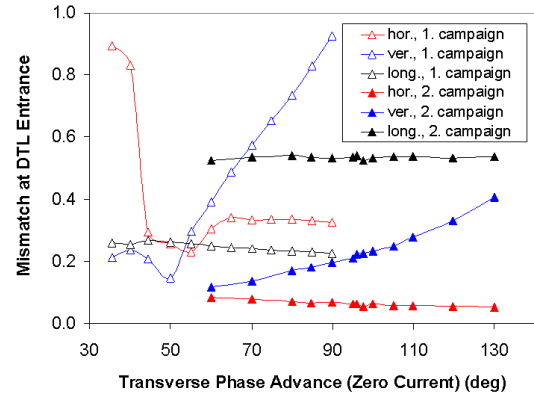


Figure 3: Mismatch between beam rms-Twiss parameters and periodic Twiss parameters at injection into the DTL as function of the phase advance  $\sigma_o$  for the two campaigns.

By defining the radius  $R$  using different powers for different sub phase spaces the halos within the planes could be modelled. Since for the longitudinal phase space distribution no measurement but on the rms-bunch length is available, a Gaussian distribution cut at  $4\sigma$  is assumed. This can be achieved by setting the respective powers in the definition of  $R$  to a value of 2. It must be mentioned that the applied method is not sensitive for eventual correlations among different planes. Such correlations have been assumed to be zero.

## MEASUREMENTS WITH MODERATE MISMATCH

The reconstructed initial distribution together with the applied setting along the matching section to the DTL was used to estimate the amount of mismatch at the DTL entry using the DYNAMION code. As shown in Fig 3 the mismatch has been very small for intermediate  $\sigma_o$  and moderate in one plane for low and for high values of  $\sigma_o$ . For the applied  $\sigma_o$  from 35° to 90° full beam transmission was observed through the DTL in the experiment. The codes revealed losses of about 2%. Figure 4 displays final horizontal phase space distributions at the DTL exit as obtained from measurements and from simulations for three different values of  $\sigma_o$ . The simulated final distributions look quite similar. Simulations could reproduce the wings attached to the core measured at highest phase advances. But the codes did not show the asymmetric distributions measured at lowest phase advances. The simulated longitudinal phase spaces showed filamentation and emittance growth due to slight rf-bucket overflow at the DTL injection. Final transverse rms-emittances are presented in Fig. 5 to Fig. 7 as function of the transverse phase advance  $\sigma_o$ . The measurements and the simulations revealed lowest emittances at  $\sigma_o \approx 60^\circ$ . In general good agreement among the codes was found. However, the codes slightly underestimate the emittance growth. This is reasonable since the codes assume a machine without errors causing additional

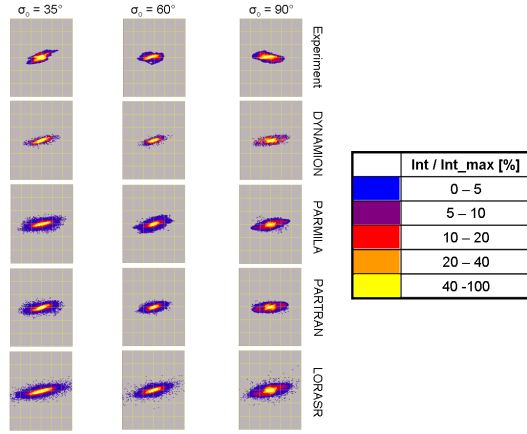


Figure 4: Top to bottom: horizontal phase space distributions at the DTL exit. Left:  $\sigma_o = 35^\circ$ ; center:  $\sigma_o = 60^\circ$ ; right:  $\sigma_o = 90^\circ$ . The scaling is  $\pm 24$  mm (horizontal axis) and  $\pm 24$  mrad (vertical axis), respectively.

growth [14].

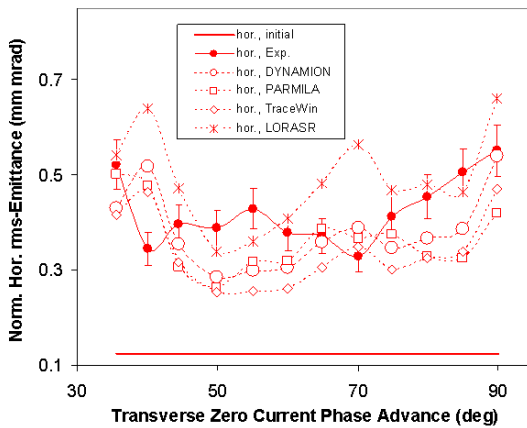


Figure 5: Horizontal rms-emittance at the end of the DTL as function of  $\sigma_o$ .

## MEASUREMENTS WITH SMALL MISMATCH

The second campaign aimed for the measurement of the  $90^\circ$  stop-band thus varying  $\sigma_o$  from  $60^\circ$  to  $130^\circ$ . It was found that the initial distribution was of the same type as during the first campaign and that its initial emittances were very similar to the previous ones as well. However, during this second campaign the mismatch to the DTL has been minimized by applying a dedicated rms-matching routine [15]. The successful reduction of mismatch (Fig. 3) is required in order to minimize effects of the envelope instability that might blur the effects of the 4<sup>th</sup>-order space charge resonance. A characteristic feature of this resonance are four wings in the transverse phase space distributions being attached to the beam core. The measurements used just the first tank of the Alvarez DTL accelerating the beam

**Beam Dynamics and Electromagnetic Fields**

**D03 - High Intensity - Incoherent Instabilities, Space Charge, Halos, Cooling**

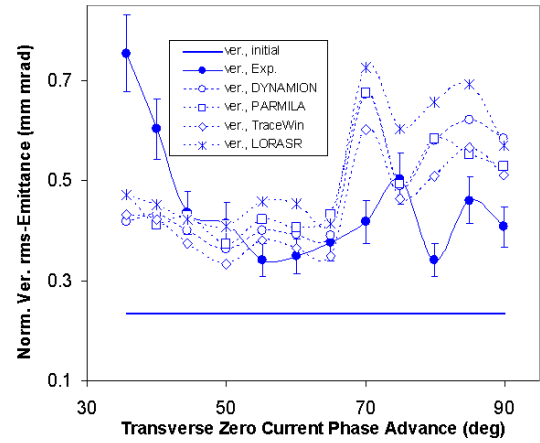


Figure 6: Vertical rms-emittance at the end of the DTL as function of  $\sigma_o$ .

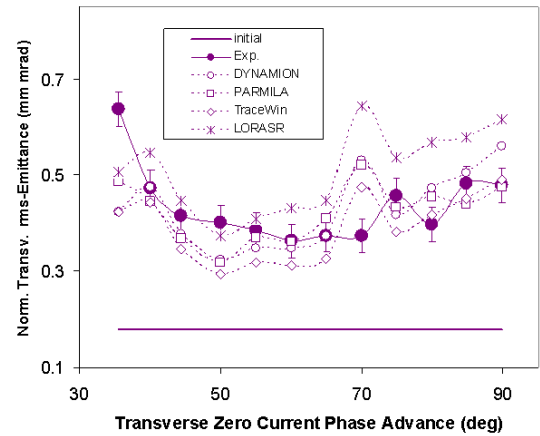


Figure 7: Mean value of horizontal and vertical rms-emittance at the end of the DTL as function of  $\sigma_o$ .

to 3.6 MeV/u, thus avoiding disturbing mismatch in the inter-tank sections. A dedicated slit/grid emittance measurement has been installed behind the first tank for these measurements.

After measuring and simulating the transverse phase space distributions at the DTL exit as plotted in Fig. 8, the corresponding rms-emittances were evaluated. The mean value of the horizontal and vertical rms-emittance, i.e.  $\epsilon_{rms,\perp} = (\epsilon_{rms,x} + \epsilon_{rms,y})/2$ , is also presented in Fig. 8 as function of the phase advance  $\sigma_o$ .

The emittance  $\epsilon_{rms,\perp}$  at the DTL exit was found to be independent of the phase advance for values of  $\sigma_o \leq 90^\circ$ . Growth was observed for  $\sigma_o \geq 90^\circ$  in both transverse planes. These observations are in very good agreement to the simulations done with three different codes. The measured growth rate of  $\epsilon_{rms,\perp}$  is constant for  $\sigma_o \geq 110^\circ$ . In the horizontal plane the measured growth disappeared for  $\sigma_o \geq 110^\circ$  while the vertical growth increased, leading to a constant growth for the mean transverse emittance  $\epsilon_{rms,\perp}$ . The codes reproduced the behavior in the horizontal plane but they delivered reduced growth beyond the resonance

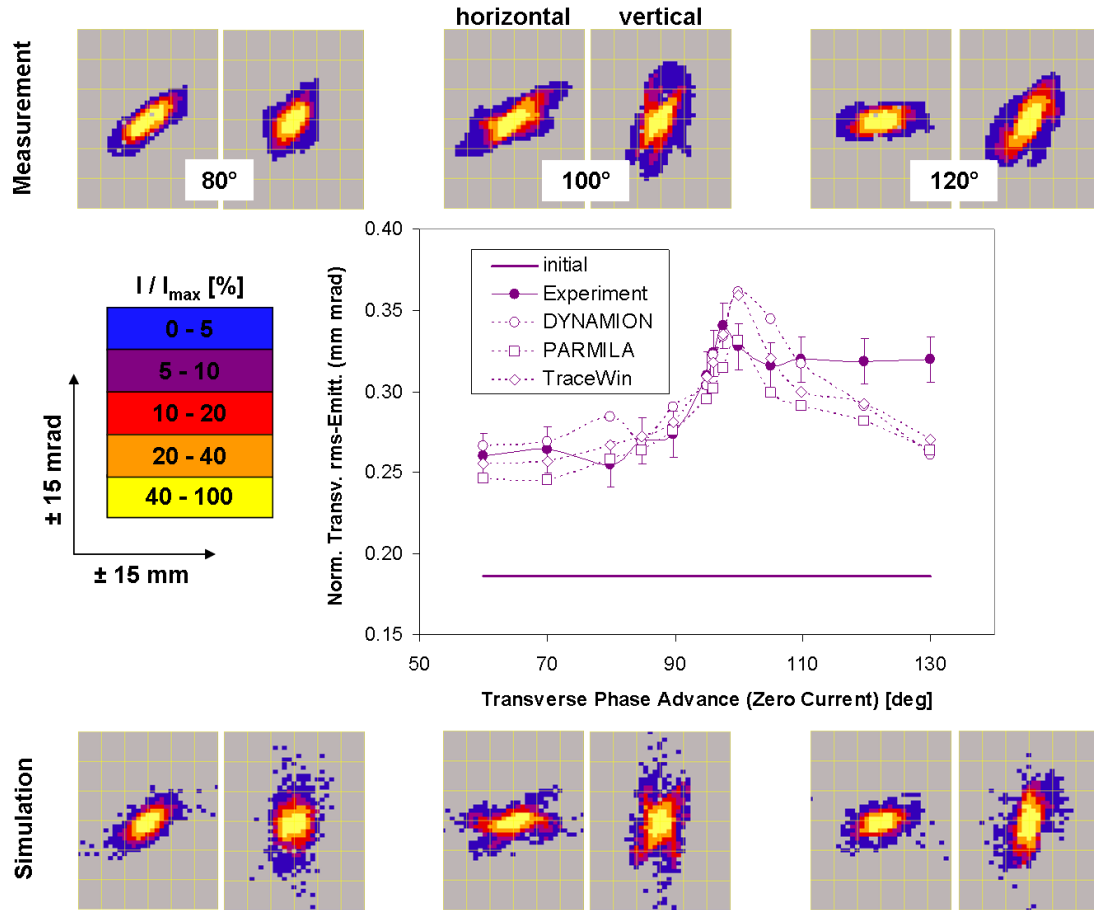


Figure 8: Upper and lower: phase space distributions at the exit of the first DTL tank as obtained from measurements and from the DYNAMION code for phase advances  $\sigma_o$  of 80°, 100°, and 120°. Left (right) side distributions refer the horizontal (vertical) plane. The scale is  $\pm 15$  mm and  $\pm 15$  mrad. Fractional intensities refer to the phase space element including the highest intensity. Center: Mean of horizontal and vertical normalized rms-emittance behind the first DTL tank as function of  $\sigma_o$ .

also in the vertical plane. This disagreement might be due to unknown residual correlations between the two transverse planes in the initial distribution being not included into the simulations as mentioned above.

Distributions corresponding to phase advances far away from the stop-band have elliptical shapes (Fig. 8). At  $\sigma_o \approx 100^\circ$  instead the measurements and the simulations clearly revealed four arms, which are typical for a resonant 4<sup>th</sup>-order interaction – here due to space charge.

This confirms the existence of a resonance stop-band as predicted in previous theoretical work [16, 11]. The experimental stop-band is well confirmed by simulation results using the actual linac structure. The exact width of the stop-band depends on the type of periodic focusing – it is zero for constant focusing. A necessary condition is  $\sigma_o \geq 90^\circ$ ; according to the theoretical analysis of [17] the width shrinks linearly to zero with the space charge tune shift  $\sigma_o - \sigma$ . In our case the stop-band width is approximately given by  $\sigma_o - \sigma \approx 20^\circ$ . For phase advances above the resonance the measurements revealed a constant  $\epsilon_{rms,\perp}$  higher than below, while the simulations predicted a de-

creasing slope. To verify whether the asymmetric behavior of  $\epsilon_{rms,\perp}$  around the resonance is due to the increased residual mismatch at higher  $\sigma_o$ , simulations with a perfectly matched beam starting at the entrance of the DTL were performed. The results revealed the same asymmetric behavior as observed in the simulation of the experiment with slightly mismatched beams.

To estimate the effect of the envelope instability, the rms-envelopes delivered by DYNAMION simulations have been evaluated. Figure 9 shows the envelopes for three different values of  $\sigma_o$ , revealing that there is no instability within the first DTL tank at 120°, i.e. at  $\sigma_o \geq 90^\circ$ . The oscillating behavior of the envelope at 100° is driven by the 4<sup>th</sup>-order resonance.

During the preparation of the experiments simulations using a KV-distribution with similar rms-emittances and equal rms-mismatch to the DTL have been done. They revealed very low rms-emittance growth of less than 10%. Since KV-distributions do not have a 4<sup>th</sup>-order space charge potential, this demonstrates that for the measured emittance growth the 4<sup>th</sup>-order resonance dominates over

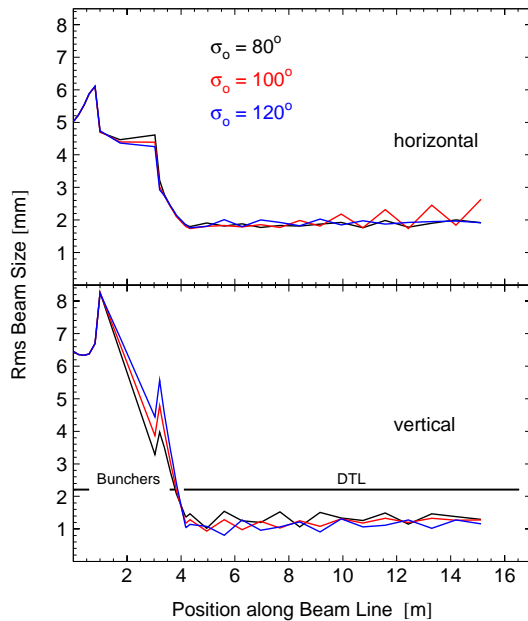


Figure 9: Rms-envelopes of the beam from DYNAMION simulations for three different transverse zero current phase advances along the DTL. Upper: horizontal; lower: vertical.

the envelope instability as predicted in [11].

Hence these measurements are the first direct evidence of a 4<sup>th</sup>-order space charge driven resonance in a linear accelerator. They thus offer a rigorous experimental basis for the 90° stop-band, which has so far been used in design consideration on theoretical grounds only.

Summarizing we found the codes reproduce well the sum of the two transverse emittances. The agreement improves with the quality of the matching to the DTL. This is plotted in Fig. 10, where the relative deviation between the measured emittances and the codes predictions is plotted versus the mean of the horizontal and transverse mismatch. For a mean mismatch of less than 20% the codes accuracies are always better than 20%, while for larger mismatches the codes might deliver final rms-emittances that differ of up to 50% from the experimental values.

### ACKNOWLEDGEMENT

We acknowledge the support of the European Community-Research Infrastructure Activity under the FP6 “Structuring the European Research Area” programme (CARE, contract number RII3-CT-2003-506395).

The participation of D. Jeon to this work was made possible partly by the support of ORNL/SNS (managed by UT-Battelle, LLC, for the U.S. Department of Energy under contract DE-AC05-00OR22725).

### REFERENCES

[1] R. Ryne et al., proc. of the Hb2008 workshop, Nashville, U.S.A. (2008).

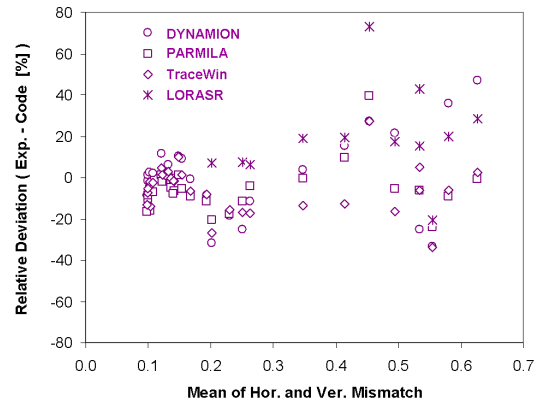


Figure 10: Relative deviation between final transverse rms-emittances as measured and predicted by the codes as function of the mean of the horizontal and the vertical mismatch to the DTL. The graph summarizes the results of the two benchmarking campaigns.

[2] S. Nath et al., Proc. of the 2001 Part. Accel. Conf., Chicago, U.S.A., (2001).

[3] A. Franchi et al., Proc. of the XXIII Linac Conf., Knoxville, U.S.A., (2006).

[4] A. Franchi et al., <http://www-dapnia.cea.fr/Phocea/file.php?class=std&&file=Doc/Care/note-2006-011-HIPPI.pdf>

[5] W. Barth et al., Proc. of the XXII Linac Conf., Lübeck, Germany, (2004).

[6] S. Yarmyshev et al., Nucl. Instrum. & Methods in Phys. Res. A **558**, 1, (2006).

[7] J.H. Billen and H. Takeda, PARMILA Manual, Report LAUR-98-4478, Los Alamos, 1998 (Revised 2004).

[8] R. Duperrier et al., ICSS 2002 Conf., Amsterdam, The Netherlands (2002).

[9] R. Tiede, PhD thesis, Goethe University Frankfurt a.M., to be published.

[10] L. Groening et al., Phys. Rev. ST Accel. Beams **11**, 094201 (2008).

[11] D. Jeon, I. Hofman, L. Groening, and G. Franchetti, in Proceedings of the XXIV Linear Accelerator Conference, Victoria, 2008.

[12] P. Forck et al., Proc. of the XX Linac Conf., Monterey, U.S.A., (2000).

[13] G. Riehl, *PROEMI: An emittance measurement and evaluation code*. The manual is available from the code author on request (g.riehl@gsi.de).

[14] K.R. Crandall, AOT Division Technical Note LA-CP-96-16, January 22, 1966.

[15] L. Groening, [http://www-linux.gsi.de/~lgroenin/bd\\_unilac/HSI/Alvarez\\_Matching.html](http://www-linux.gsi.de/~lgroenin/bd_unilac/HSI/Alvarez_Matching.html).

[16] I. Hofmann, G. Franchetti, and A. Fedotov, in *Proceedings of the AIP Conference* **642**, 2002, edited by AIP, p. 248.

[17] I. Hofmann, L.J. Laslett, L. Smith, and I. Haber, Part. Acc. **13**, 145 (1983).